Author(s): Kettunen, Heikki; Uusitalo, Juha; Leino, Matti; Jones, Peter; Eskola, Kari; Greenlees, Paul; Helariutta, Kerttuli; Julin, Rauno; Juutinen, Sakari; Kankaanpää, Harri; Kuusiniemi, Pasi; Muikku, Maarit; Nieminen, Päivi; Rahkila, Panu

Title: Alpha-decay studies of the nuclides 195Rn and 196Rn

Year: 2001

Version: Published version

Please cite the original version:

Kettunen, H., Uusitalo, J., Leino, M., Jones, P., Eskola, K., Greenlees, P., Helariutta, K., Julin, R., Juutinen, S., Kankaanpää, H., Kuusiniemi, P., Muikku, M., Nieminen, P., & Rahkila, P. (2001). Alpha-decay studies of the nuclides 195Rn and 196Rn. Physical Review C, 63(4), Article 044315. https://doi.org/10.1103/PhysRevC.63.044315

α decay studies of the nuclides ^{195}Rn and ^{196}Rn

H. Kettunen,[1] J. Uusitalo,[1] M. Leino,[1] P. Jones,[1] K. Eskola,[2] P. T. Greenlees,[1] K. Helariutta,[1,*] R. Julin,[1] S. Juutinen,[1] H. Kankaanpää,[1] P. Kuusiniemi,[1] M. Muikku,[1] P. Nieminen,[1] and P. Rahkila[1]

[1]*Department of Physics, University of Jyväskylä, P.O. Box 35, FIN-40351 Jyväskylä, Finland*

[2]*Department of Physics, University of Helsinki, FIN-00014 Helsinki, Finland*

(Received 22 December 2000; published 16 March 2001)

The new neutron deficient nuclide ^{195}Rn and the nuclide ^{196}Rn have been produced in fusion evaporation reactions using ^{56}Fe ions on ^{142}Nd targets. A gas-filled recoil separator was used to separate the fusion products from the scattered beam. The activities were implanted in a position sensitive silicon detector. The isotopes were identified using spatial and time correlations between implants and decays. Two α decaying isomeric states, with $E_\alpha = 7536(11)$ keV [$T_{1/2} = (6^{+3}_{-2})$ ms] for the ground state and $E_\alpha = 7555(11)$ keV [$T_{1/2} = (5^{+3}_{-2})$ ms] for an isomeric state were identified in ^{195}Rn. In addition, the half-life and α decay energy of ^{196}Rn were measured with improved precision. The reduced widths deduced for the neutron deficient even-mass Rn isotopes suggest an onset of substantial deformation at $N = 110$.

DOI: 10.1103/PhysRevC.63.044315 PACS number(s): 21.10.Dr, 23.60.+e, 27.80.+w

I. INTRODUCTION

Very low production rates of neutron deficient heavy translead nuclei in heavy ion reactions often exclude in-beam γ-ray measurements. Alpha decay then provides the only viable means to obtain spectroscopic information. The latest study of the very neutron deficient Rn isotopes was performed by Pu *et al.* [1]. Their identification of the new α decaying isotope ^{196}Rn was based on three correlated recoil $-\alpha-\alpha$ chains where the second α decay in the chain had decay properties characteristic of ^{192}Po. The Rn isotope ^{197}Rn was studied by Enqvist *et al.* [2]. Following the systematics of odd-mass Rn isotopes in the region below $N = 126$, two α decaying isomeric states ($I^\pi = 13/2^+$ and $I^\pi = 3/2^-$) were identified. The neighboring nuclide ^{198}Rn is the most neutron deficient Rn isotope for which in-beam γ-ray studies have been carried out [3].

Very recently detailed α decay fine structure studies have been performed for the neutron deficient Po isotopes ^{191}Po [4–6] and ^{192}Po [7,8] (daughter activities of the Rn isotopes studied in this work). The isotope ^{191}Po was studied at the Jyväskylä gas-filled recoil separator RITU [9] utilizing the $\alpha-\gamma$ coincidence technique at the separator focal plane [4,6]. Two α decaying isomeric states were observed with $E_\alpha = 7334(5)$ keV and $T_{1/2} = 22(1)$ ms [$I_\alpha = 77(3)\%$] assigned to the $3/2^-$ ground state of ^{191}Po and $E_\alpha = 7376(5)$ keV and $T_{1/2} = 93(3)$ ms [$I_\alpha = 50(3)\%$] assigned to the $13/2^+$ isomeric state of ^{191}Po. In addition, decay lines with $E_\alpha = 6966(10)$ keV [$I_\alpha = 8(3)\%$] and $E_\alpha = 6888(5)$ keV [$I_\alpha = 46(4)\%$], feeding the excited $3/2^-$ and $13/2^+$ states in ^{187}Pb^m and ^{187}Pb^g, respectively, were observed. In fact, it turned out that the 6888 keV α decay is unhindered (hindrance factor HF=0.63) and the 7376 keV α decay is strongly hindered (HF=26). As discussed in Ref. [6] the 93 ms $13/2^+$ state is believed to be an oblate deformed isomeric very pure $\nu i_{13/2} \otimes [\pi(4p-2h)]_{0^+}$ intruder state while the 22 ms $3/2^-$ state is an admixture of the spherical $\nu p_{3/2} \otimes [\pi(2p-0h)]_{0^+}$ and deformed $\nu p_{3/2} \otimes [\pi(4p-2h)]_{0^+}$ configurations.

The α decay of ^{192}Po was studied recently in Jyväskylä utilizing the $\alpha-e^-$ coincidence technique at the separator focal plane [7]. Two excited 0^+ states in ^{188}Pb were observed to be fed by α decay in addition to the ground state to ground state decay. The fine structure decays, feeding the $\pi(2p-2h)$ and $\pi(4p-4h)$ 0^+ states in ^{188}Pb, turned out to be more favored than the ground state to ground state 0^+-0^+ decay. In this case the interpretation is that the ^{192}Po 0^+ ground state contains a strong $\pi(4p-2h)$ intruder configuration component associated with weak oblate deformation. Similar fine structure in the α decay has so far been identified in six different even-mass Po isotopes [7,10–12].

II. EXPERIMENTAL DETAILS

Heavy ion induced fusion evaporation reactions of the type ^{142}Nd(^{56}Fe,xn)$^{198-x}$Rn were used to synthesize neutron deficient Rn isotopes in three separate experiments in the present work. The ^{56}Fe beam was produced by the $K = 130$ MeV cyclotron of the Accelerator Laboratory at the Department of Physics of the University of Jyväskylä (JYFL). The metal ions made by the volatile compounds (MIVOC) method [13] developed at JYFL was used to produce the iron beam from the ECR ion source. The fine adjustment of the bombarding energies was performed using a set of nickel and carbon foils in front of the target. Energy losses in the degrader foils, in the gas window, in the targets, and in the helium gas filling were calculated using the TRIM code [14]. Ten different bombarding energies, varying from 239 to 267 MeV, were used. Typical beam intensities were 10–30 pnA and the total beam on target time was 300 h. Targets of rolled Nd of thickness between 0.5 and

*Present address: Gesellschaft für Schwerionenforschung, D-64220 Darmstadt, Germany.

1.0 mg/cm^2 were used. The isotopic composition of the target by mass number was the following: ^{142}Nd 98.26%, ^{143}Nd 0.71%, ^{144}Nd 0.58 %, ^{145}Nd 0.12%, ^{146}Nd 0.24%, ^{148}Nd 0.05%, and ^{150}Nd 0.04%.

The nuclides ^{196}Rn and ^{195}Rn studied in this work were produced in rather cold $2n$ and $3n$ fusion evaporation channels. By minimizing the number of evaporation steps the losses due to the strong fission competition are reduced. Also the number of open reaction channels and therefore unwanted contaminants are reduced when bombarding energies close to the Coulomb barrier are used.

Evaporation residues resulting from fusion reactions were separated from the beam using the JYFL gas-filled recoil separator RITU. After passing through a multiwire proportional avalanche gas counter (MWPAC) the residues were implanted into a position sensitive silicon detector placed 10 cm behind the avalanche gas counter at the focal plane of RITU. The silicon detector (305 μm thick) is divided into 16 position sensitive strips and the total area of the detector is 35×80 mm^2. Since the vertical position resolution of each strip is better than 500 μm the silicon detector can be treated as a pixel detector of more than 1000 pixels. Using spatial and time correlation, the implants were linked with their subsequent α decays and with decays of their daughter nuclei. The gas counter was used to separate the α particles from the low energy recoils. The recoil energy loss in the gas counter combined with the recoil energy deposited in the silicon detector could be used to separate the candidate fusion evaporation products from the scattered beam particles. The pressure of the helium filling gas in RITU was typically 100 Pa. The RITU gas volume was separated from the high vacuum of the beam line using a 50-μg/cm^2 carbon foil. The counting gas in the gas counter was isobutane of 300 Pa and the counter windows, made of 120-μg/cm^2 mylar, were also used to keep the silicon detector chamber in high vacuum. The silicon detector was cooled down to 253 K using circulating alcohol. The events were gain matched and calibrated using well known α activities produced in the bombardments and in one of the experiments by using a separate reaction with the ^{56}Fe beam on a ^{106}Cd target. The aim of the use of the ^{106}Cd target was to produce known α activities with high α particle energies with sufficient yields. For the energy calibration the α particle energies were taken from Refs. [15,16] when a ^{142}Nd target was used and from Ref. [17] when a ^{106}Cd target was used. The full width at half maximum value with all the 16 strips summed up was measured to be 30 keV at the α energy of 7000 keV.

III. RESULTS

Figure 1(a) presents the energy spectrum of all decays observed in the silicon detector and vetoed with the gas counter using the ^{56}Fe+^{142}Nd reaction with all bombarding energies combined. The spectrum is dominated by activities formed in fusion channels involving charged particle evaporation. In Fig. 1(b) only decays correlated within 100 ms with the implanted residues inside the proper recoil energy gates are shown. Thus the faster decaying activities are enhanced. Figure 1(c) shows decays with the additional requirement that the decays are followed within 1 s by α particles with energies between 6000 and 8000 keV. The activity ^{195}At [18] is enhanced in addition to those higher energy events which mostly belong to Rn isotopes produced in xn fusion evaporation channels. Finally in Fig. 2 a two-dimensional energy plot is shown where the different isotopes can be recognized. Two groups which belong to ^{195}At can clearly be seen. In addition, several neutron deficient Rn isotopes can be identified. The heavier Rn isotopes were produced due to the heavier Nd isotopes in the target enriched in ^{142}Nd.

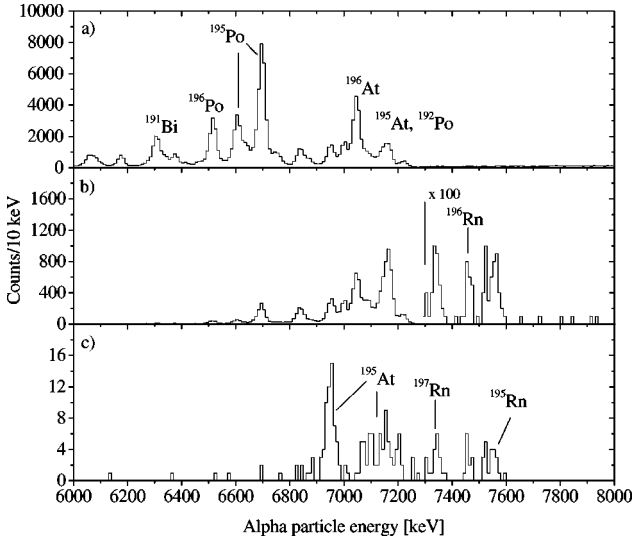

FIG. 1. Energy spectra of α particles measured in the silicon detector and vetoed with the gas counter using the ^{56}Fe+^{142}Nd reaction: (a) all decays; (b) decays following recoil implants within 100 ms; (c) decays followed, in addition, by 6000–8000-keV α particles within 1 s.

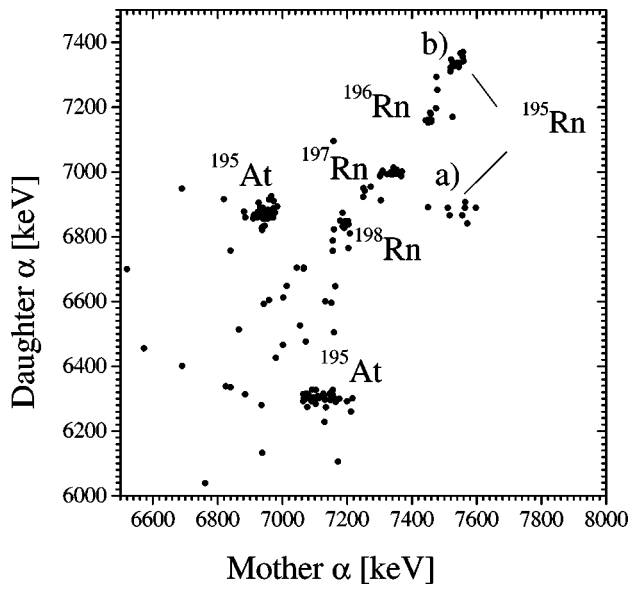

FIG. 2. Mother and daughter α particle energies for all chains of the type ER$-\alpha_m-\alpha_d$ observed in the ^{56}Fe+^{142}Nd irradiation. Maximum search times were 100 ms for the ER$-\alpha_m$ pair and 1 s for the $\alpha_m-\alpha_d$ pair.

TABLE I. The measured α decay properties. The literature values are taken from Refs. [1,6,16]. For ^{196}Rn and ^{195}Rn the hindrance factors and half-lives normalized to ^{212}Po are calculated according to Ref. [21]. For ^{191}Po the hindrance factors are taken from Ref. [6].

Nuclide	E_α [keV]	E_α [keV]	$T_{1/2}$ [ms]	$T_{1/2}$ [ms]	$T_{1/2}$ [ms]	HF
	Meas.	Lit.	Meas.	Lit.	Calc.	
^{196}Rn	7461(9)	7492(30)	$4.4^{+1.3}_{-0.9}$	3^{+7}_{-2}	15	1
^{192}Po	7167(11)	7167(7)	29^{+15}_{-8}	33.2(14)	25	1
^{195}Rn^m	7555(11)		5^{+3}_{-2}		8	2.1
^{191}Po^m	7364(20)	7376(5)	95^{+130}_{-60}	93(3)		26
^{191}Po^m	6878(12)	6888(5)	110^{+70}_{-30}	93(3)		0.63
^{195}Rn^g	7536(11)		6^{+3}_{-2}		9	2.2
^{191}Po^g	7331(11)	7334(5)	15^{+7}_{-3}	22(1)		2.9

In total nine ER$-\alpha_m-\alpha_d$ decay chains (ER refers to evaporation residue, α_m and α_d refer to the mother α and daughter α decays, respectively) assigned to the isotope ^{196}Rn were observed. The measured α-particle energy $E_\alpha=7457(12)$ keV and half-life $T_{1/2}=(3.4^{+1.8}_{-0.9})$ ms, of the mother activity are compatible with those reported in Ref. [1], where an energy of $E_\alpha=7492(30)$ keV and a half-life of $T_{1/2}=(3^{+7}_{-2})$ ms are given. The mother activity was followed by a daughter activity with $E_\alpha=7167(11)$ keV and $T_{1/2}=(29^{+15}_{-8})$ ms. The daughter activity is identified as ^{192}Po for which the decay properties of $E_\alpha=7167(7)$ keV and $T_{1/2}=33.2(14)$ ms [8] have been reported. Taking into account all the identified nineteen ER$-\alpha_m$ chains with proper α particle energy the decay properties of $E_\alpha=7461(9)$ keV and $T_{1/2}=(4.4^{+1.3}_{-0.9})$ ms are determined for the isotope ^{196}Rn.

In the case of ^{195}Rn the identification is more complicated. In the work of Ref. [4] three strong α particle decays were reported for the activity ^{191}Po (daughter activity in this work). One of those α particle decays can be seen in the two dimensional spectrum shown in Fig. 2 group (a). The measured daughter activity energy $E_\alpha=6878(12)$ keV and half-life $T_{1/2}=(110^{+70}_{-30})$ ms are compatible with the decay properties $E_\alpha=6888(5)$ keV and $T_{1/2}=93(3)$ ms reported for ^{191}Po^m [6]. This daughter activity was preceded by an activity with decay properties of $E_\alpha=7555(13)$ keV and $T_{1/2}=(3^{+2}_{-1})$ ms which therefore could be identified to originate from the new Rn isotope ^{195}Rn^m. Altogether seven such ER$-\alpha_m-\alpha_d$ chains were identified.

The group (b) in Fig. 2 can be divided into two parts. The first part includes 11 ER$-\alpha_m-\alpha_d$ chains and the second part has in total three ER$-\alpha_m-\alpha_d$ decay chains. The mother activities with $E_\alpha=7536(11)$ keV and $T_{1/2}=(6^{+3}_{-2})$ ms and $E_\alpha=7555(20)$ keV and $T_{1/2}=(9^{+12}_{-4})$ ms were followed by daughter activities with $E_\alpha=7331(11)$ keV and $T_{1/2}=(15^{+7}_{-3})$ ms and $E_\alpha=7364(20)$ keV and $T_{1/2}=(95^{+130}_{-60})$ ms, respectively. The measured decay properties for the daughter activities are compatible with the values of $E_\alpha=7334(5)$ keV and $T_{1/2}=22(1)$ ms and $E_\alpha=7376(5)$ keV and $T_{1/2}=93(3)$ ms reported for ^{191}Po^g and ^{191}Po^m, respectively [6]. Therefore the mother activities are assigned to ^{195}Rn^g and ^{195}Rn^m, respectively.

The above division of the decay events in group (b) into two parts is based on the two α particle energies (7376 and 7334 keV) measured for ^{191}Po in the work of Ref. [6] from where it can be seen that the α particle energies are 42 keV apart from each other. This energy difference is bigger than the energy resolution measured for the detector setup used in this work. After this division it can be seen that the measured lifetimes indeed support this assignment. Even though the number of chains is only three in the second group the measured average lifetime 137 ms for this daughter activity is far too long to be arising from the 22 ms ^{191}Po^g group.

It is quite unlikely that the observed lifetimes of the daughter nuclei in these 14 decay chains originate from only one nuclear species. Making this assumption, however, one arrives at the half-life of (32^{+12}_{-7}) ms for the daughter activity. While this result is not in strong disagreement with the known half-life of 22(1) ms for ^{191}Po^g, it would be highly unlikely to observe the long lifetimes 157 and 226 ms when the sample size is only 14 decays. One can also determine the probability that the observed width of the lifetime distribution is due to only one decaying source [19]. The resulting relatively small value of 17% is compatible with our assumption that both ^{191}Po^g and ^{191}Po^m contribute to the daughter decays.

Finally the second group and the activity followed by the 6878-keV α decay can be combined and the decay properties of $E_\alpha=7555(11)$ keV and $T_{1/2}=(5^{+3}_{-2})$ ms are proposed to belong to ^{195}Rn^m.

The energy resolution of the detector setup was not good enough that the determined α decay energy difference (7555–7536 keV) 19 keV could clearly be seen in the singles α particle decay spectra although the α particle decay energy distribution assigned to ^{195}Rn is wider than that assigned to ^{196}Rn [see Figs. 1(b) and (c)]. Also the measured two half-lives are too close to each other to allow any firm conclusions to be made and therefore the identified ER$-\alpha_m$ chains which were not followed by the second α with full energy are not included in the final decay properties of ^{195}Rn given in Table I. The predicted partial β-decay half-lives $\sim$2.5 and $\sim$1.7 s for ^{196}Rn and ^{195}Rn [20], respectively, are much longer than the measured half-lives and, hence, α branching ratios $b_\alpha\approx1$ are assumed.

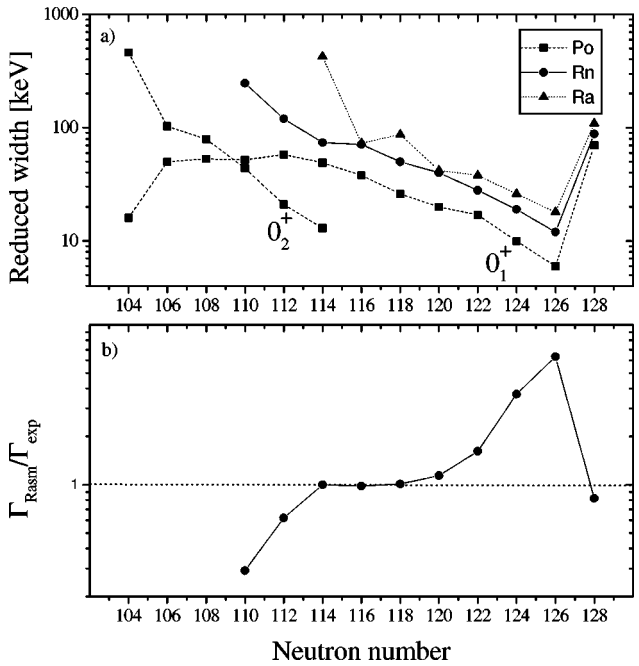

FIG. 3. (a) Reduced α decay width values of neutron deficient isotopes of Po, Rn, and Ra. The filled squares represent values determined for Po, the filled circles represent values determined for Rn, and the filled triangles represent values determined for Ra. (b) Calculated α decay width relative to measured α decay width for neutron deficient isotopes of Rn.

The efficiency of the RITU separator was not measured but an assumed value of 30% should give cross sections accurate to within a factor of 2. Both isotopes ^{196}Rn and ^{195}Rn were produced with peak cross sections of about 2 nb.

IV. DISCUSSION

Through systematic study of α decay hindrance factors HF and reduced widths δ^2 important structure information on the decaying states is obtained. In the present work the experimental reduced α decay widths were determined according to Rasmussen [21]. The reduced α decay widths for neutron deficient even-mass Po, Rn, and Ra isotopes are shown in Fig. 3(a). A gradual increase in the reduced width values is considered to be a normal feature with increasing neutron deficiency. The Po isotopes are an exception. The reduced widths for the ground state to ground state transitions remain constant for even-mass Po isotopes lighter than ^{196}Po and even decrease significantly for ^{188}Po. The reason for this is that the α decays from the Po 0^+ ground states to the proton $(2p-2h)$ 0^+ intruder states in Pb nuclei are getting increasingly favorable. This feature is shown in Fig. 3(a) where also reduced widths for decays between Po ground states and 0_2^+ intruder states in Pb are shown. These low excitation $\pi(2p-2h)$ states are associated with oblate deformation. The interpretation has been given that the ground states of neutron deficient Po isotopes are mixtures of different configurations, spherical $\pi(2p-0h)$, oblate $\pi(4p-2h)$ [and prolate $\pi(6p-4h)$].

Based on the δ^2 values shown in Fig. 3(a) the following observation concerning the Rn isotopes can be made. The reduced α decay widths of even-mass Rn isotopes with neutron numbers of $114 \leqslant N \leqslant 126$ increase smoothly with decreasing neutron number. The reduced α decay width value for ^{198}Rn is slightly higher and the α decay width value of ^{196}Rn is clearly higher than the smooth behavior predicts. These α decays are relatively more favored than the α decays of the heavier even-mass Rn neighbors. Presumably the α decay from a normal configuration to the intruder configuration will be at least slightly hindered. Because the daughter activities (^{192}Po and ^{194}Po) are shown to have intruder configurations in their ground states the same should be true also in ^{196}Rn and ^{198}Rn. Therefore, for example, the 0^+ ground state in ^{196}Rn contains a strong $\pi(6p-2h)$ intruder configuration and the α decay occurs from this state to the 0^+ ground state in ^{192}Po having a strong $\pi(4p-2h)$ intruder configuration. This is also in good agreement with the recent in-beam γ-ray studies where the same kind of intruder structures were exposed for ^{198}Rn, ^{194}Po, and ^{192}Po [3,22].

It is intriguing that the α decays of ^{198}Rn and ^{196}Rn seem to be clearly faster than the smooth behavior of heavier even-mass Rn isotopes predicts. This is illustrated in Fig. 3(b) where the ratio of calculated and experimental absolute α decay widths $\Gamma_{Rasm}/\Gamma_{exp}$ $(\Gamma=\hbar\lambda)$ for even-mass Rn isotopes are shown. The half-lives were calculated according to Rasmussen [21] and normalized to ^{212}Po. It is characteristic that the partial α decay half-lives of the spherical nuclei at the magic neutron number 126 are underestimated. Starting from neutron number 120 the calculated α-decay half-lives agree well with the experimental ones until starting from neutron number 112 (^{198}Rn) the half-lives are clearly overestimated.

In a simple picture it should be easier for an α particle to penetrate out from the poles of the nucleus than from the equator if the nucleus has a prolate deformed (nonspherical) shape and the overall effect will be a higher penetration probability. The corresponding reasoning also applies to oblate deformed nuclei. For example, in the work by Delion *et al.* [23], absolute α decay widths $(\Gamma=\hbar\lambda)$ with regard to the level of deformation were studied. The experimental decay widths were well reproduced for deformed nuclei when theoretical decay widths were calculated assuming a deformed Coulomb barrier. One feature shown was that the calculated decay rates are faster through a deformed Coulomb barrier than through a spherical Coulomb barrier. The final conclusion is therefore that especially in the case of ^{196}Rn the α decay is taking place between deformed (and strongly mixed) 0^+ ground states.

The α decay of ^{202}Ra is also anomalously fast as can be seen from Fig. 3(a). The measured decay properties of ^{202}Ra [24] are based on one event and therefore the statistical error is large. But this case could also be a sign of α particle decay between deformed (and mixed) ground states.

The hindrance factor is defined as the ratio of the reduced width of the ground state to ground state transition in the closest even-even neighbor to the reduced width of the transition in question. In odd-mass nuclei a hindrance factor of less than 4 implies an unhindered decay between states of

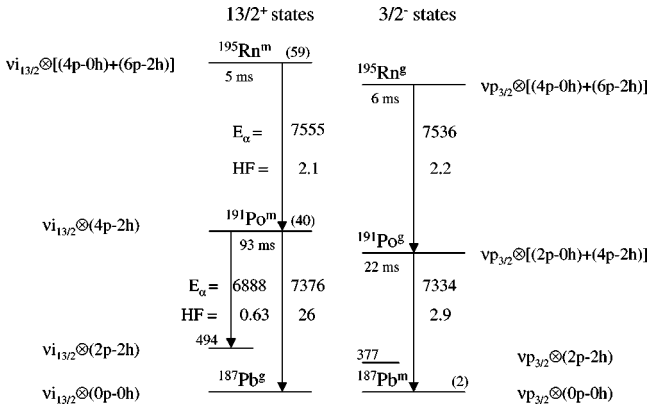

FIG. 4. Proposed α decay scheme of $^{195}Rn^{m,g}$. Only the α decays seen in this work are shown. All the data and interpretations belonging to ^{191}Po are taken from Ref. [6].

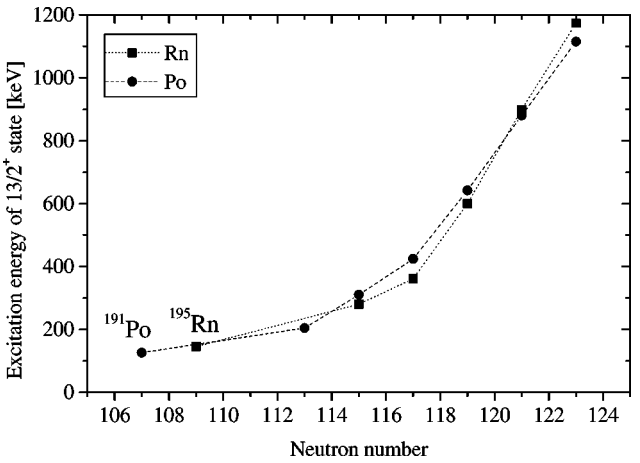

FIG. 5. The experimental $13/2^+$ energies with regard to the ground state of neutron deficient isotopes of Po and Rn.

equal spin, parity, and configuration [25]. Hindrance factors for the isotope ^{195}Rn determined in this work in addition to those taken from Ref. [6] for the daughter activity ^{191}Po are shown in Table I. The hindrance factors of $^{195}Rn^{m}$ and $^{195}Rn^{g}$ lead to the conclusion that the α decays occur between states of equal spin, parity, and configuration. Thus the 7536 keV α decay originates from the $3/2^-$ ground state of ^{195}Rn and the 7555 keV α decay from the $13/2^+$ isomeric state of ^{195}Rn. This isomeric state lies about 59 keV above the ground state based on the reported corresponding level spacing in the daughter nucleus ^{191}Po [6]. Here one should remember that in ^{191}Po the $13/2^+$ isomeric state is believed to be an oblate deformed isomeric very pure $\nu i_{13/2}\otimes[\pi(4p-2h)]_{0^+}$ state while the $3/2^-$ state is an admixture of the spherical $\nu p_{3/2}\otimes[\pi(2p-0h)]_{0^+}$ and deformed $\nu p_{3/2}\otimes[\pi(4p-2h)]_{0^+}$ configurations [6]. Therefore the hindrance factors of about 2 indicate that the intruder component is also strongly present in both of the corresponding states in ^{195}Rn. In Fig. 4 the proposed decay scheme of ^{195}Rn together with data for the daughter is shown. This scheme fits well with the measured systematics of heavier odd-mass Rn isotopes for which a falling trend of energy of the isomeric $13/2^+$ state with regard to the ground state $3/2^-$ (or $5/2^-$) as a function of decreasing neutron number has been observed. This behavior is illustrated in Fig. 5 where the energies of $13/2^+$ isomeric states with regard to the ground states in Rn and Po isotopes ($N\leqslant 123$) are shown.

In Fig. 6 the experimental α decay Q values of Rn isotopes with neutron number $N\leqslant 127$, including ^{195}Rn and ^{196}Rn studied in this work, are compared with those calculated using the mass tables of Liran and Zeldes [26], obtained using a semiempirical shell-model mass formula, and of Möller *et al.* [27], obtained using macroscopic-microscopic calculations. As can be seen from Fig. 6, the Liran and Zeldes α decay Q values fit the experimental data rather well, especially when moderately neutron deficient isotopes are considered. It is interesting to note the bigger deviations in the Q_α values at mass 200 in the Möller *et al.* prediction due to the predicted onset of deformation for Rn nuclei, whereas the daughter nuclei (Po) are predicted to be almost spherical [27].

In Ref. [28], mass excesses of $-17760(100)$ keV and $-32330(100)$ keV were reported for ^{188}Pb and ^{179}Pt, respectively, utilizing Schottky mass spectrometry. These nuclei are connected through α particle decay chains to Rn isotopes studied in this work. Using the reported α particle decay energies of ^{183}Hg [15], ^{187}Pb [29], ^{191}Po [6], and ^{195}Rn a mass excess of 4990(110) keV is obtained for ^{195}Rn. Correspondingly, using the α decay energies of ^{192}Po [16] and ^{196}Rn a mass excess of 2020(110) keV is obtained for ^{196}Rn. For comparison, a mass excess of 2150(200) keV was recommended for ^{196}Rn in the latest mass evaluation of Audi and Wapstra [30].

In conclusion, the α particle decay properties of the new isotope ^{195}Rn were investigated for the first time, and the α decay of ^{196}Rn was studied with improved accuracy. The determined reduced α decay widths indicate a $\Delta l=0$ character for the observed transitions. An unexpectedly fast de-

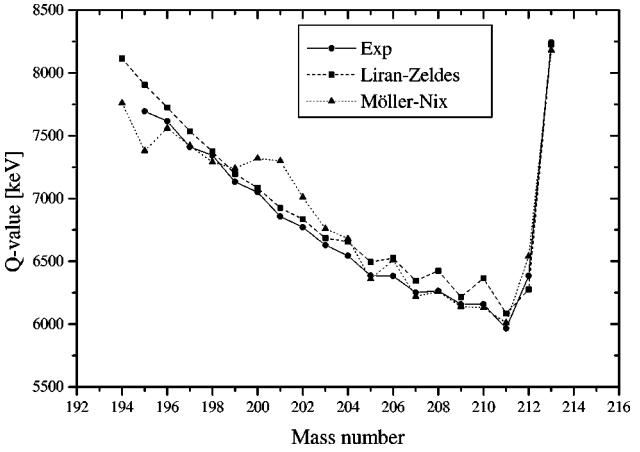

FIG. 6. α decay Q values of neutron deficient isotopes of Rn. The filled circles represent data, including the α decay Q values for ^{195,196}Rn deduced in this work. The filled squares and triangles represent α decay Q values calculated using mass tables by Liran and Zeldes and by Möller *et al.*, respectively.

cay rate measured for the isotope ^{196}Rn could be a sign of a significant ground state deformation in this nucleus. It is striking to note that the α decay properties of ^{195}Rn and ^{196}Rn point to the same characteristics of the decaying states as their corresponding daughter activities ^{191}Po and ^{192}Po have.

ACKNOWLEDGMENT

This work was supported by the Academy of Finland under the Finnish Center of Excellence Program 2002-2005 (Project No. 44875, Nuclear and Condensed Matter Physics Program at JYFL).

[1] Y. H. Pu *et al.*, Z. Phys. A **357**, 1 (1997).
[2] T. Enqvist, P. Armbruster, K. Eskola, M. Leino, V. Ninov, W. H. Trzaska, and J. Uusitalo, Z. Phys. A **354**, 9 (1996).
[3] R. B. E. Taylor *et al.*, Phys. Rev. C **59**, 673 (1999).
[4] A. N. Andreyev *et al.*, Phys. Rev. Lett. **82**, 1819 (1999).
[5] A. N. Andreyev *et al.*, in *Experimental Nuclear Physics in Europe*, edited by B. Rubio, M. Lozano, and W. Gelletly, AIP Conf. Proc. No. 495 (AIP, Melville, NY, 1999), p. 121.
[6] A. N. Andreyev *et al.* (unpublished).
[7] R. G. Allatt *et al.*, Phys. Lett. B **437**, 29 (1998).
[8] N. Bijnens *et al.*, Z. Phys. A **356**, 3 (1996).
[9] M. Leino *et al.*, Nucl. Instrum. Methods Phys. Res. B **99**, 653 (1995).
[10] J. Wauters *et al.*, Phys. Rev. Lett. **72**, 1329 (1994).
[11] A. N. Andreyev *et al.*, Eur. Phys. J. A **6**, 381 (1999).
[12] A. N. Andreyev *et al.*, Nature (London) **405**, 430 (2000).
[13] H. Koivisto, J. Ärje, and M. Nurmia, Nucl. Instrum. Methods Phys. Res. B **94**, 291 (1994).
[14] J. F. Ziegler, J. P. Biersack, and U. Littmark, *The Stopping and Range of Ions in Solids* (Pergamon, New York, 1985).
[15] A. Rytz, At. Data Nucl. Data Tables **47**, 205 (1991).
[16] J. Wauters, P. Dendooven, M. Huyse, G. Reusen, P. Van Duppen, P. Lievens, and ISOLDE Collaboration, Phys. Rev. C **47**, 1447 (1993).
[17] R. D. Page, P. J. Woods, R. A. Cunningham, T. Davinson, N. J. Davis, A. N. James, K. Livingston, P. J. Sellin, and A. C. Shotter, Phys. Rev. C **53**, 660 (1996).
[18] M. Leino *et al.*, Acta Phys. Pol. B **26**, 309 (1995).
[19] K. H. Schmidt, Eur. Phys. J. A **8**, 141 (2000).
[20] P. Möller, J. R. Nix, and K.-L. Kratz, At. Data Nucl. Data Tables **66**, 131 (1997).
[21] J. O. Rasmussen, Phys. Rev. **113**, 1593 (1959).
[22] K. Helariutta *et al.*, Eur. Phys. J. A **6**, 289 (1999).
[23] D. S. Delion, A. Insolia, and R. J. Liotta, Phys. Rev. C **54**, 292 (1996).
[24] M. Leino *et al.*, Z. Phys. A **355**, 157 (1996).
[25] Nucl. Data Sheets **15**, No. 2, VI (1975).
[26] S. Liran and N. Zeldes, At. Data Nucl. Data Tables **17**, 431 (1976).
[27] P. Möller, J. R. Nix, W. D. Myers, and W. J. Swiatecki, At. Data Nucl. Data Tables **59**, 185 (1995).
[28] T. Radon *et al.*, Nucl. Phys. **A677**, 75 (2000).
[29] P. Misaelides *et al.*, Z. Phys. A **301**, 199 (1981).
[30] G. Audi and A. H. Wapstra, Nucl. Phys. **A595**, 409 (1995).